RSC Advances

ROYAL SOCIETY OF CHEMISTRY

www.rsc.org/advances

Content entry

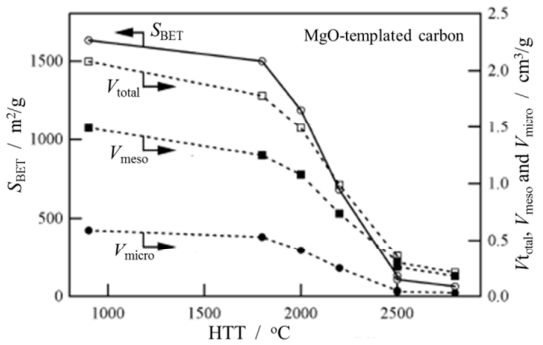

Control of crystallinity by high temperature treatment and catalytic carbonization is reviewed on porous carbons from different precursors and processes.

RSC Advances

RSCPublishing

REVIEW

Control of crystalline structure of porous carbons

Cite this: DOI: 10.1039/x0xx00000x

Received ooth January 2012,
Accepted ooth January 2012

DOI: 10.1039/x0xx00000x

www.rsc.org/

Michio Inagaki*[a] Masahiro Toyoda[b] and Tomoki Tsumura[b]

The control of crystalline structure in porous carbons by high temperature treatment and catalytic carbonization is reviewed, after a brief review on the control of pore structure. The development of crystallinity and the preservation of porous structure in porous carbons by high temperature treatment depend predominantly on carbon precursors. The experimental results published are summarized, which are suggested the necessity of more detailed and systematic investigations.

1. Introduction

Porous carbons are widely used in various fields from private houses to industrial factories for the remediation of the living environment and of the working circumstance, and the improvement of the qualities of products. Activated carbons have been used since prehistoric era and have been representing porous carbons. With increasing application fields for activated carbons, however, the requirements for the porous carbons became severe, not only large specific surface area but also specific pores with a sharp size distribution. To meet the requirements for different applications, various carbonization techniques have been proposed and studied extensively,[1,2] such as designing carbon precursors, carbonization using various templates, etc., as summarized in Table 1. In addition to optimize the pore structure for applications, high electrical conductivity and high crystallinity of porous carbons are strongly demanded in some applications; high conductivity is preferable for the electrodes of electrochemical capacitors to reduce its internal resistivity in order to have better performances,[3] high crystallinity of activated carbon fibres gives better conversion efficiency from NO to NO_2 at room temperature,[4] etc. In order to fulfil these requirements, the development of graphite structure in porous carbons is essential, for that either high-temperature treatment of porous carbons or catalytic carbonization using metals has been tried (Table 1).

In the present review, controls of pore and crystalline structures of porous carbons, are reviewed. A brief summary on the control of pore structure in carbon is presented here, because pore structure control in carbon materials has been reviewed in a number of journals and books[1-14], and also because these processes influences on the improvement in crystalline structure of carbon. The control of crystalline structure in porous carbons has not yet been reviewed, as the authors concern, although the development of crystalline structure (graphitization) in various carbon materials has been studied and reviewed by numerous researchers. The graphitization behaviour of porous carbons is expected to be a little different from that reported for different carbon materials, such as graphitizing and non-graphitizing carbons, mainly because the graphitization occurs in a limited space of pore walls, and is far from the complete understanding. In the present review, therefore, the emphasis is placed on crystalline structure control in porous carbons, although the studies in a wide range of conditions and detailed analyses are very rare in the published papers.

[a] Professor Emeritus of Hokkaido University, 228-7399 Nakagawa, Hosoe-cho, Kita-ku, Hamamatsu 431-1304, Japan E-mail: im-ii@ace.ocn.ne.jp

[b] Faculty of Engineering, Oita University, 700 Dannoharu, Oita 870-1192, Japan

Table 1 Processes to control pore and crystalline structures in carbon materials

Control of pore structure	
Activation	Opening closed pores existed and enlarging pore size.
Selection of carbon precursor	Designing and control in molecular structure of precursors
Template carbonization	Various templates (zeolites, silicas, block copolymer surfactants, MOFs, MgO, metal carbides, etc.)
Carbon fibre mats	Nonwoven mats of carbon fibres and nanofibers
Control of crystalline structure	
High temperature treatment	Heat treatments above 2000 °C for the development of graphitic structure
Catalytic carbonization	Various metals (Fe, Ni, Co, etc.) by mixed into carbon precursors Improvement in crystallinity during carbonization (below 1500 °C)

2. Pore structure control

Activation, of which fundamental chemical reaction is oxidation involving gasification to CO and CO_2, has been used in industries to produce activated carbons.[1,5,6] Activation process has been classified into two; chemical activation using air, steam, etc. and physical activation using $ZnCl_2$, KOH, etc. as activation agents. Extremely high surface area, as high as 3600 m^2/g, was obtained by using KOH[15] and activation by using alkaline hydroxides was reviewed.[16] Change in pore structure during activation of a glass-like carbon spheres by using air is demonstrated as Fig. 1, revealing that pore size is enlarged with activation from ultra-micropore (with the size of less than 0.7 nm) to mesopore (2~50 nm) through super-micropore (0.7~2 nm), in other words, enlarged with sacrificing the smaller-sized pores.[17] By prolonged activation, mesopores change to macropores (larger than 50 nm) by sacrificing mesopores, being accompanied by the reduction of the yield of porous carbon.

Nanoporous carbons have been prepared from some specific precursors only via simple carbonization; defluorination of poly(tetrafluoro-ethylene),[18,19] carbonization of some polyimides containing pendant groups[20] and carbonization of aerogels.[21,22] Nanoporous carbon membranes with molecular sieving characteristics were prepared by the carbonization of various polyimides: including commercially available Kapton[23-25] and polyetherimide,[26,27] and others.[28-30] Polyimides containing pendant groups $-CH_3$ and $-CF_3$ in their repeating units gave microporous carbons by single-step carbonization at 600 °C.[31,32] In Fig. 2a, microporous surface area S_{micro} determined from α_s plot for the carbon membranes prepared from fluorinated aromatic polyimides (Fig. 2b) is plotted against fluorine content;[22] formation of micropores in the carbon membrane depends strongly on the content of fluorine-containing pendant groups and the polyimide membrane containing 31.3 mass% F gives microporous surface area S_{micro} of about 1340 m^2/g and micropore volume V_{micro} of 0.44 cm^3/g with a sharp size distribution peak at about 0.55 nm. Defluorination of poly(tetrafluoroethylene) (PTFE) with Na metal gives mesopore-rich carbon and a high S_{BET} as 2225 m^2/g.[33]

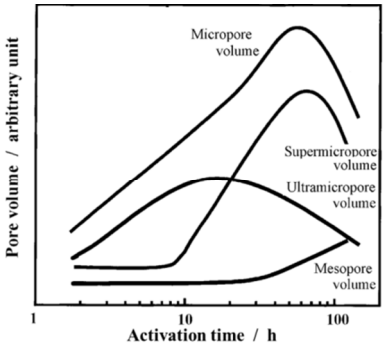

Fig. 1 Relative changes in volumes of different pores, ultramicro-, supermicro- and meso-pores in a glass-like carbon spheres.[7]

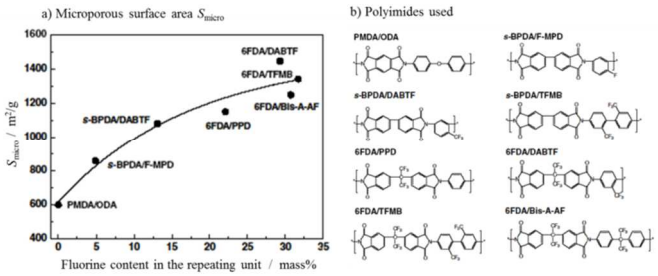

Fig. 2 Change in microporous surface area S_{micro} with fluorine content in polyimide repeating unit; (a) S_{micro} vs. fluorine content, b) Molecular structure of polyimides. Reproduced from ref. 32 with permission.

Various templating techniques to control pore structure in carbon materials without any activation process have been proposed, mainly because of more exact control of pore structure and avoidance of sacrificial loss of carbon atoms. Microporous carbons have been prepared by carbonization using zeolites,[34,35]

metal-organic frameworks (MOFs)[36] and metal carbides[37-39] as templates. Mesoporous carbons were prepared by using mesoporous silicas,[40,41] block copolymer surfactants,[42,43] colloidal silicas[44-48] and MgO[49-51] as templates, and macropores by using organic foams[52-56] as templates. Templates and carbon precursors, which have been employed, are summarized with the resultant pore structures and typical values of surface area and volume of pores, in addition with template performance in Table 2. Template carbonization was reviewed from different viewpoints.[10-13,57-59]

The carbons prepared by using zeolite templates are highly microporous, as shown in Table 3, the impregnation of poly(furfuryl alcohol), followed by CVD of propylene at 700 °C, and then heat-treatment at 900 °C resulting in exceptionally high S_{BET} of 3600 m^2/g and a large V_{micro} of about 1.5 cm^3/g.[60] Micropores in zeolite-templated carbons are ordered and have uniform size, because of inheritance of the pore structure in zeolite. Chlorination of metal carbides gives microporous carbon without any additional carbon precursor and any activation process, as shown in Fig. 3 by comparing pore size distribution for the carbons derived from different carbides.[61] One of MOFs (metal-organic-frameworks), MOF-5 ($Zn_4O(O_2CC_6H_4CO_2)_3$), could give microporous carbon with S_{BET} of 1800 m^2/g and V_{total} of 2.87 cm^3/g[62] and MOF-5 impregnated by furfuryl alcohol and carbonized at 1000 °C gave S_{BET} of 2872 m^2/g and V_{total} of 2.06 cm^3/g.[63] Metallic Zn produced by pyrolysis of MOF-5 was vaporized out above its boiling point (908 °C) to leave porous carbon. Zeolite-type MOF (ZIF-8, $Zn(C_4H_5N_2)_2$) gave the carbon having more developed pore structure after impregnation of furfuryl alcohol vapor.[64]

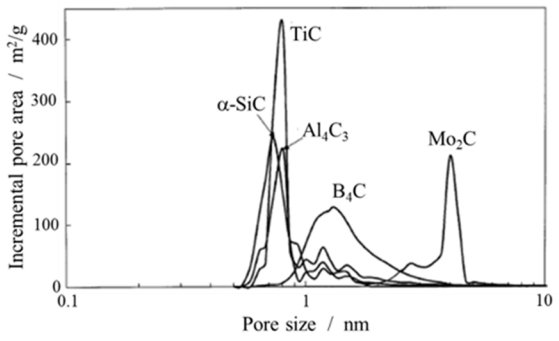

Fig. 3 Pore size distribution of microporous carbons derived different carbide. Reproduced from ref. 61 with permission.

Mesopore-rich carbons are prepared from different carbon precursors by using mesoporous silicas (MCM-48, SBA-15, etc.), triblock copolymer surfactants (F127, P123, etc.), colloidal silicas, and MgO as templates. Mesopores in the carbons prepared via templating of mesoporous silicas and triblock copolymer surfactants are ordered and some of them are channels having the diameters corresponding to mesopores. Mesopores formed via colloidal silica spheres are very homogeneous size and sometimes well aligned. However, mesopores formed via MgO template have relatively homogeneous size, but not be aligned. It has to be pointed out that the template MgO can be recycled.[65]

3. Crystalline structure control

3.1 High temperature treatment

Since the development of nanotexture in carbon materials by carbonization and that of crystalline structure by heat treatment above 2000 °C depends strongly on their precursors,[1] the papers reporting the results of high temperature treatment of porous carbons are summarized on different carbon precursors in Table 4, by listing carbonization processes, high temperature treatment conditions, and brief summary of the experimental results. For commercially available activated carbons, the precursor and its carbonization conditions are not described in the table.

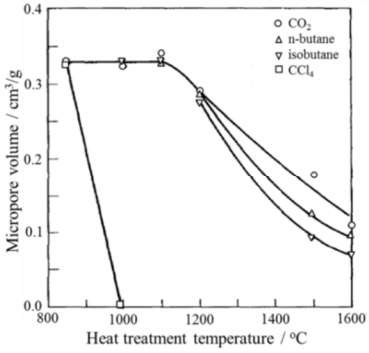

Fig. 4 Dependence of micropore volumes determined by different gases on heat treatment temperature. Reproduced from ref. 66 with permission.

For activated carbon prepared from Akabira coal by carbonization at 850 °C for 8 h in a stream and following heat treatment at 1000-1600 °C for 1/4 h, the adsorption isotherms of CO_2, n-butane, isobutane, and CCl_4 were determined at 298 K.[66] V_{micro} determined by

different gases, except CCl_4, decrease rapidly with increasing heat treatment temperature (HTT) above 1100 °C and V_{micro} determined by CCl_4 became zero even at 1000 °C, as shown in Fig. 4. Considering that kinetic diameter of CO_2, n-butane, isobutane and CCl_4 is 0.33, 0.43, 0.50 and 0.60 nm, respectively, the carbon shows a marked performance for molecular sieving after the heat treatment at 1000 °C. Marked decreases in microporous surface area S_{micro} and V_{micro} were reported on commercially available activated carbons.[67-71] Marked reduction in S_{micro} from 890 m^2/g for the pristine activated carbon to 62 m^2/g after 1900 °C treatment was observed.[68] Marked reductions of surface areas determined by different methods were observed from adsorption/desorption isotherm of benzene vapor at 293 K on an activated carbon, as shown in Fig. 5.[69] Change in pore structure with HTT was discussed on the bases of Brunauer-Emmett-Teller (BET), Dubinin-Radshkevicz (DR), Dubinin-Astakhov (DA), Dubinin-Stoeckli (DS) and Horvath-Kawazoe (HK) theories. After 2100 °C-treatment, 002 diffraction profile shifts to high angle side (apparent interlayer spacing d_{002} of 0.342 nm) and sharpened. 002 diffraction profile shown in the paper looks like to be composite of at least two peaks, broad peak at low-angle-side and one at sharp high-angle-side, although the authors do not pay attention it.[69] Increase in residence time at 1100 °C up to 6 h causes a slight decrease in S_{BET} determined by Ar adsorption at 87 K.[71] The adsorption isotherms were analysed on the bases of finite and infinite wall thickness models.

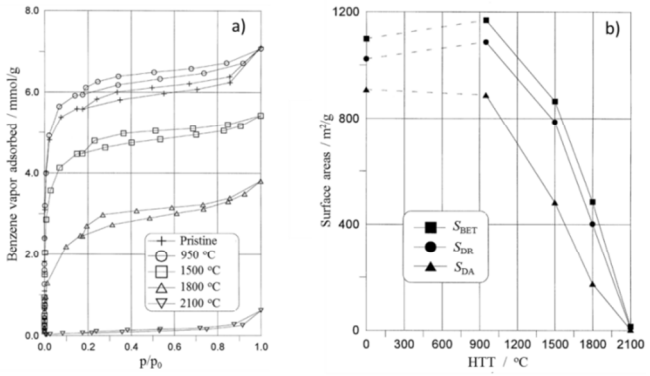

Fig.5 Changes in adsorption/desorption isotherms (a) and surface areas determined by BET, DR and DA methods (b) with HTT for an activated carbon. Reproduced from ref. 69 with permission.

Table 2 Template carbonization techniques for pore structure control in carbons.

Templates			Carbon precursors	Carbon prepared		Template performance	
				Pore structure	Pore surface area & volume	Removal	Cycl-ability
In-organic	Zeolites	Zeolite Y, β and L, ZSM-5	Propylene, CVI + FA, impregnation	Micropores ordered	3700 m^2/g, 1.8 cm^3/g 4000 m^2/g, 1.8 cm^3/g	HF or NaOH	No
	Meso-porous silicas	MCM-48, MCM-41, SBA-1 and SBA-15	Sucrose, FA, PF and MP, impregnation. Acetylene, CVI,	Mesopores ordered or disordered	1130 m^2/g~1.0 cm^3/g 1520 m^2/g, 1.3 cm^3/g	HF or NaOH	No
	Colloidal silicas	Organic silicates and inorganic silica	Mixing with RF, AN,	Micro- & meso-pores disordered	1512 m^2/g, 3.6 cm^3/g 2600 m^2/g, 1.4 cm^3/g	HF	No
	MgO	MgO, Mg acetate, citrate, $Mg(OH)_2$	Mixing with PVA, coal tar pitches, PET, PIs	Mesopores disordered	1800 m^2/g 1600 m^2/g, 1.7 cm^3/g	Acetic or citric acids	Easy recycle
	Metal carbides	B_4C, SiC, Ti_2AlC, TiC, Mo_2C	Not necessary	Ultramicro-pores disordered	3100 m^2/g, 1.66 cm^3/g	Vaporiza-tion as chlorides	No
Metal-organic	MOFs	(Zn_4O $(O_2CC_6H_4CO_2)_3$)	With or without FA	Mesopores, disordered	2872 m^2/g, 2.06 cm^3/g	Not needed	No

Organic	Surfact-ants	Diblock & triblock copolymers	Mixing with RF, EOA, PGF, AN	Mesopores ordered or disordered	1354 m^2/g, 0.74 cm^3/g 968 m^2/g, 0.56 cm^3/g	Not needed	No
	Organic foams	Urethane & melamine foams	Impregnation of PIs	Macro- & micropores	1540 m^2/g, 0.63 cm^3/g	Not needed	No

CVI: chemical vapour infiltration, FA: furfuryl alcohol, PF: phenol formaldehyde, MP: mesophase pitch, RF: resolcinol-formaldehyde, AN: acrylonitrile, PVA: poly(vinyl alcohol), PET: poly(ethylene terephthalate), PIs: polyimides, EOA: triethyl orthoacetate, PGF: phloroglucinol-formaldehyde

Table 3 Pore structure parameters of the carbons prepared by zeolite template (courtesy of Prof. T. Kyotani of Tohoku University).

Templating conditions			Pore structure parameters of templated carbon		
Carbon precursor	Template zeolite	Carbonization conditions	S_{BET} (m^2/g)	V_{micro} (cm^3/g)	V_{meso} (cm^3/g)
PAN	NaY	700 °C, 3 h	580	0.28	0.10
PFA	NaY	700 °C, 3 h	590	0.28	0.15
Propylene	USY	700 °C, 18 h	2260	1.11	0.76
		800 °C, 15 h	2200	0.88	0.83
PFA + Propylene	Y	700 °C, 4 h	2170	0.9	0.4
		700 °C, 4 h + 900 °C 3h	3600	1.5	0.0

Table 4 Papers reporting the results of high temperature treatment of porous carbons

Carbonization		Heat treatment condition	Summary of experimental results	Ref
Carbon precursor	Process			
Activated carbon prepared from coal at 850°C		1000, 1100, 1200, 1500, 1600 °C	V_{micro} evaluated from different gases show no appreciable change up to 1100°C.	66
Carbon molecular sieve		850-1400°C for 1h	Studied on molecular sieving of O_2 and Ar.	67
Activated carbon (Norit RO 0.8)		1300, 1900 °C for 2h	Studied as a support in iron catalysts for NH, synthesis.	68
Activated carbon (Norit R3-ex)		950-2100°C for 1/6h	Analyses by BET, DA, DS and HK theories.	69
Activated carbon (Norit ROX 0.8)		1300-1500°C for 1h	Rapid decrease in S_{micro} by heat treatment.	70
Activated carbon (Norit R1 Extra)		1100°C for 1, 2 and 6h	Rapid disappearance of ultramicropores	71
Kraft lignin	Carbonization at 1100°C	1400- 2800°C	Above 2400°C, two components, graphite and turbostratic structures	72
Sucrose	Silica templates (SBA-15	1500-2500°C for 1.5h	Rapid decreases in S_{BET} and pore volumes with	73

	and MCM-48) at 900°C	in Ar	HTT	
Resorcinol/ formaldehyde	Carbon aerogel, 1000°C for 4 h	1600-2800°C for 0.5h	Micropore disappeared at 2000°C and 50% mesopores are remained after 2800 °C	74
Resorcinol/ formaldehyde	Soft templating (F127) at 850°C	1800-2600°C for 1h	Considerable mesoporosity is maintained after 2600°C	75
Phenol resin	Nano-sized SiO_2 with surfactant (F127) at 700°C	1200°C in N_2	Compared with commercial mesoporous carbon fibre and microporous activated carbon	77
Phloroglucinol/ formaldehyde	Soft templating (F127) at 850°C for 2h	2200°C for 1h	As the support for metal particles for CO hydrogenation to ethanol.	76
Poly(furfuryl alcohol)	Oxidation at 900 °C to 84% burn-off	1200-2000°C for 1h	After 2000°C-treatment, S_{BET} of 1060m^2/g and composite X-ray profile of A, T and G.	80
Mesophase pitch	Colloidal SiO_2 particles, at 900°C	2400°C for 2h	Preservation of the shape of mesopores and retaining the high surface area	81
Mesophase pitch	Colloidal SiO_2 crystals, 1000°C	2500°C for 0.5h	Ordered mesoporous structure consisting of straight fringes after 2500°C-treatment.	82
Mesophase pitch	Colloidal SiO_2 particles, 1000°C.	1000-2500°C	Preservation of mesoporosity, applied as anode material for LIB.	83
Mesophase pitch	Silica template (SBA-15) at 900°C	1200-2400°C for 2h	Anode performance in Lithium-ion batteries	84
Petroleum pitch	Silica templates (SBA-15 & MCM-48) at 950 °C	1200°C for 10 h and then 1400°C for 4 h	Structural regularity is preserved upon heat treatment at 1400°C.	85
Poly(vinyl chloride)	Silica templates (SBA-15 and MSU-1) at 800°C	2300°C for 0.5h	Relatively high surface area (SBET of 260 m^2/g) and mesopores of 2-15 nm size	86
Poly(vinyl alcohol) (PVA)	MgO templating at 900°C	1800-2800°C for 1h	Highly porous structure with S_{BET} of 1600 m^2/g was almost unchanged even at 2000 °C.	89
PVA	MgO templating at 900°C	1000-2800°C for 1h	Studied for electrode materials in lithium-ion capacitor	90
PVA	MgO templating at 900°C	1000-3000°C for 1h	Marked decrease in S_{BET} above 2000°C, applicability to anode of lithium-ion battery	91
poly(p-phenylene benzobisoxazole) (PBO)	PBO fibres at 900 °C, CO_2 activation with burn-off of 15 and 51 mass%	1600-2700°C	Graphitization above 2400°C, d_{002} decreasing below 0.339 nm and marked decrease in surface area and pore volume	96
Methane	CVD into silica template (SBA-15), 700-1000°C	1200°C for 2h	High V_{meso}, walls of oriented carbon layer Application to batteries and supercapacitors.	92
Titanium carbide	Chlorination at 600°C, annealing at 600°C in H_2	1000-2000°C in vacuum	Vacuum annealing increases pore volume and surface area of CDC, reaching 2000 m^2/g,	94

Effect of heat treatment on porous carbons derived from biomasses, lignin[72] and sucrose,[73] were studied. The carbon produced from kraft lignin at 1100 °C and contained 2.9 mass% ash was heat-treated at 1400-2800 °C for 1 h.[72] S_{BET} decreased markedly above 1400 °C and 002 diffraction profile becomes composite above 2400 °C, which seemed to consist of two components having d_{002} of 0.342 and 0.336 nm. Ordered mesoporous carbons were prepared from sucrose using silica templates (SBA-15 and MCM-48) at 900 °C and heat-treated at 1500-2500 °C for 1.5 h.[73] In Fig. 6, relative S_{BET} (relative to the pristine) is plotted against HTT for mesoporous carbons[73] in comparison with two activated carbons[66,69] and lignin-derived carbon,[72] revealing that S_{BET} starts to decrease by the heat treatment at 1100 °C and becomes almost zero at 2500 °C commonly for activated carbons and biomass-derived carbons.

High temperature treatment was performed on porous carbons; carbon aerogels from resorcinol/ formaldehyde,[74] carbons from resorcinol/formaldehyde and phloroglucinol/formaldehyde using soft template F127,[75,76] and carbon from phenol/formaldehyde by mixing with silica nanoparticles.[77] On carbon aerogels, marked disappearance of micropores above 2000 °C and stability of mesopores up to 2800 °C are demonstrated,[74] as shown in Fig. 7. Pore structure change in carbon aerogel with HTT was also discussed by referring to immersion density using cyclohexane. Mesoporous carbons prepared by soft templating (F127) from resolcinol/ and phloroglucinol/formaldehyde also showed certain preservation of mesopores up to 2200-2600 °C.[75,76] Mesoporous carbon was prepared from thermosetting phenol resin and nano-sized silica particles by adding a surfactant (F127) to modify the surface property of the silica particles, followed by carbonization at 700 °C,[78] of which mesopores were preserved after 1200 °C treatment.[67] Carbon, which was prepared from poly(furfuryl alcohol) at 900 °C and activated by CO_2 up to the burn-off of 84 mass%, kept relatively high S_{BET} and V_{meso} of 1060 m^2/g and 0.22 cm^3/g, respectively, even after the heat treatment at 2000 °C, in comparison to the pristine carbon prepared at 850 °C (2135 m^2/g and 0.35 cm^3/g, respectively).[79,80] The 2000 °C-treated carbon gave composite 002 diffraction profile, which was analyzed to be composed of three structural components having different d_{002} as 0.366, 0.344 and 0.337 nm.

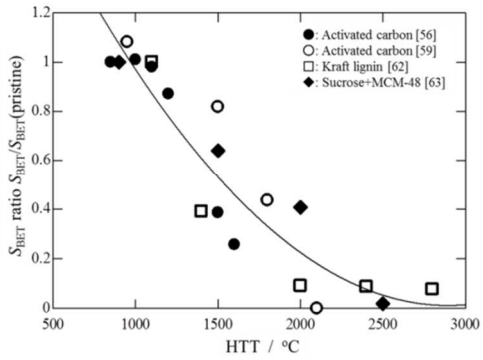

Fig. 6 Changes in S_{BET} with HTT for activated carbons and biomass-derived carbons.

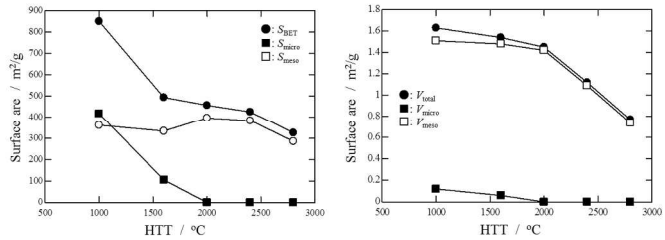

Fig. 7 Changes in surface areas and pore volumes for carbon aerogel (courtesy of Prof. Y. Hanzawa of Chiba Institute of Technology).

From pitches, porous carbons were prepared using colloidal silica (so-called imprinting method)[46,81,82] and mesoporous silica templates (SBA-15, MCM-48).[73,76,83-85] Mesophase pitch was frequently used as carbon precursor for achieving high crystallinity after high temperature treatment.[81-83] Heat treatment of the mesoporous carbon having S_{BET} of 425 m^2/g, V_{total} of 1.53 cm^3/g and homogeneous pore size of 24 nm caused the reduction to 239 m^2/g, 0.72 cm^3/g and 16.5 nm, respectively, after the treatment at 2400 °C for 2 h, in contrast to the case of saran-derived microporous carbon which changed from 1200 to 0.4 m^2/g.[81] Using silica colloidal crystal (colloid's size of about 69 nm), ordered mesoporous carbon was obtained at 1000 °C.[82] The treatment of the carbon at 2500 °C for 0.5 h gave sharp 002 diffraction line with d_{002} of 0.34 nm together with three-dimensional line 101, slight reductions in S_{BET} from 185 to 115 m^2/g and in V_{total} from 1.63 to 1.12 cm^3/g, and relatively long straight 002 lattice fringes by preserving ordered pore structure, as shown in Fig. 8. Mesoporosity evaluated by external surface area S_{ext} was kept even after the treatment at 2500 °C for mesoporous carbon prepared from coal-derived mesophase pitch using colloid silica particles (80 nm

diameter) at 1000 °C.[83] Effect of high temperature treatment was studied on mesoporous carbons prepared using mesoporous silica templates from mesophase pitch[84] and petroleum pitch.[73,85] Carbon having ordered and channel-like mesopores was prepared using mesoporous silica (SBA-15) template at 900 °C, of which pore wall consists of oriented small carbon layers, as shown in Fig. 9a and b.[84] With increasing HTT, carbon layers grow and the number of stacked layers increased (Fig.9c and d). Improvement of crystallinity was also proved by XRD and Raman spectroscopy. Both S_{BET} and V_{total} decreased with increasing HTT, S_{BET} decreasing from 167 m^2/g for 1200 °C to 3 m^2/g for 2400 °C. Ordered mesoporous carbon prepared from a petroleum pitch using SBA-15 gave S_{BET} of 923 m^2/g and V_{total} of 0.6 cm^3/g after the carbonization at 950 °C. It could keep mesoporous structure even after the treatment at 1200 °C for 10 h (S_{BET} of 784 m^2/g), but decreases markedly by the heat treatment at 1400 °C to 0.5 cm^3/g.[85]

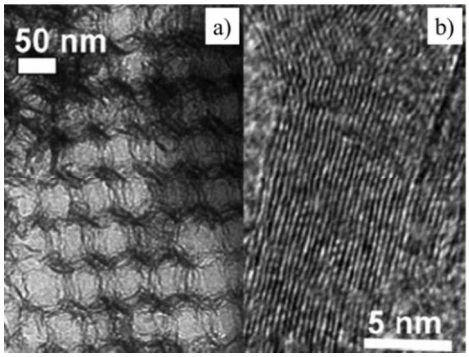

Fig. 8 Ordered mesoporous carbon prepared from a pitch via colloidal silica template after 2500 °C-treatment. Reproduced from ref. 82 with the permission of American Chemical Society.

Mesoporous carbons were prepared by using the precursors giving graphitizing carbons with templates; poly(vinyl chloride) (PVC) with mesoporous silica[86] and poly(vinyl alcohol) (PVA) with MgO.[49,65,87-91] As shown XRD patterns in Fig. 10a, the carbons prepared from PVC at 800 °C by using mesoporous silica templates (MSU-1 and SBA-15) have much better organization, well-defined diffraction peaks, but their porous structures are less-developed than those from furfuryl alcohol;[86] S_{BET} for the former are 930-950 m^2/g but that for the latter reaches 1790 m^2/g. The structure of the former is improved by the heat-treatment at 2300 °C for 0.5 h, as shown in Fig. 10b, but S_{BET} decreases to 260 m^2/g, of which the structure is still turbostratic: d_{002} of 0.342 nm and unsymmetrical 10 and 11 diffraction peaks. It has to be pointed out, however, that the profile of 002 diffraction of Fig. 10b looks composite.

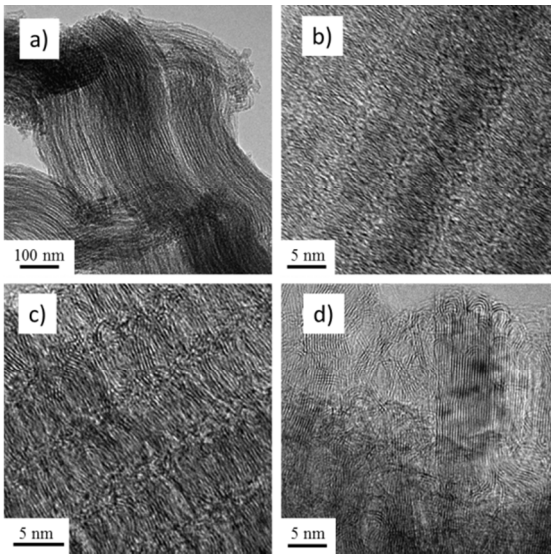

Fig. 9 Mesoporous carbon prepared from mesophase pitch via SBA-15 templating and heat-treated at different temperatures: a) and b) 1200, c) 1800 and d) 2400 °C. Reproduced from ref. 84 with permission.

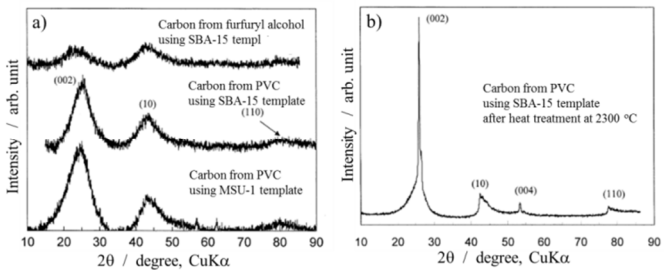

Fig. 10 XRD patterns of templated carbons from PVC and furfuryl alcohol. Reproduced from ref. 86 with permission.

Effect of heat treatment up to 2800 °C was extensively studied for the mesoporous carbons prepared by using MgO template from PVA at 900 °C.[89-91] MgO-templated carbons consist mainly of hollow nanoparticles with a size of 5-10 nm, of which the thickness of pore walls is several nanometres, as demonstrated in Fig. 11a. With the heat treatment above 1800 °C, its 00*l* diffraction profiles change to be composite. The composite 00*l* diffraction profiles are reasonably divided into three components with d_{002} of 0.343, 0.339 and 0.336 nm, as shown 004 diffraction profile of 2500 °C-treated carbon in Fig. 11d, of which structure is supposed to be turbostratic, intermediate and graphitic, respectively. Apparently two kinds of aggregates are recognized under TEM, one is shown as

1 in Fig. 11c, which is predominant and composed of hollow nanoparticles, as shown in Fig. 11b, and the other shown as **2** in Fig. 11c is an aggregate of large-sized flakes. The size of hollow nanoparticles does not change markedly even after 2800 °C treatment, but lattice fringes in their walls became much longer and were contrasted clearer. Relative contents of the components with d_{002} of 0.339 and 0.336 nm increased with increasing temperature and residence time of heat treatment. Pore parameters, S_{BET}, V_{total}, V_{micro} and V_{meso}, of the carbon are plotted against HTT in Fig. 12.[89] All pore parameters decrease markedly above 1800 °C. Electrical resistivity, which was measured on the sheet (100 μm thick) formed from the carbon powder using Teflon binder (10 mass%) by compression, decreased markedly by high temperature treatment, $3x10^{-6}$ S/cm for as-prepared carbon, $3x10^{-2}$ S/cm after 2000 °C treatment and $5x10^{-1}$ S/cm after 2500 °C treatment. S_{BET} values reported on MgO-templated carbons in three different laboratories[89-91] revealed very similar change with HTT.

Mesoporous carbons were prepared by CVD of CH_4 in mesoporous silica SBA-15 at 900 °C for different times of 0.5-3.0 h and heat-treated at 1000 and 1200 °C before and after removal of the silica template.[92] Lamellar nanotexture in pore walls, in addition to mesoporous structure being characteristic for SBA-15-templated carbon, is observed in TEM images shown in Fig. 13. By the heat treatment at 1200 °C after the removal of silica template, the carbon preserved the lamellar characteristics in TEM images, and S_{BET} of about 586 m^2/g and V_{total} of 1.27 cm^3/g with a broad pore-size distribution in mesopore range (3.7-5.0 nm) due to partial destruction and coalescence of ordered mesopore-sized channels. It has to be pointed out that lamellar texture observed in TEM cannot be a direct proof for the development of graphite structure and also that the carbons have strong D-band in Raman spectrum after 1200 °C treatment, although the authors have used the terms "graphitized" and "graphitic nature".

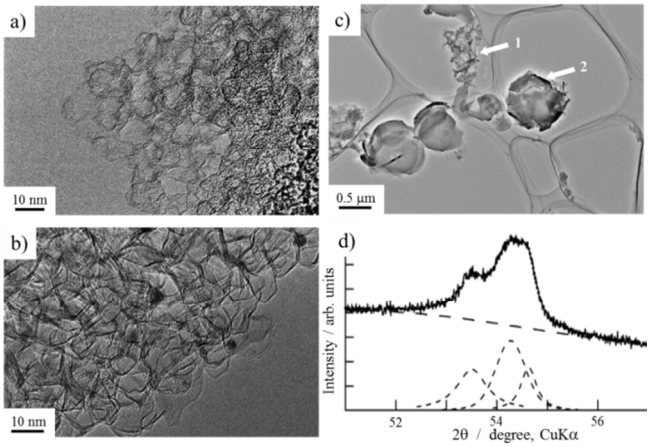

Fig. 11 TEM images and 004 diffraction profile of MgO-templated carbons: a) as-prepared, b - d) after the treatment at 2500 °C for 5 h. Reproduced from ref. 89 with permission.

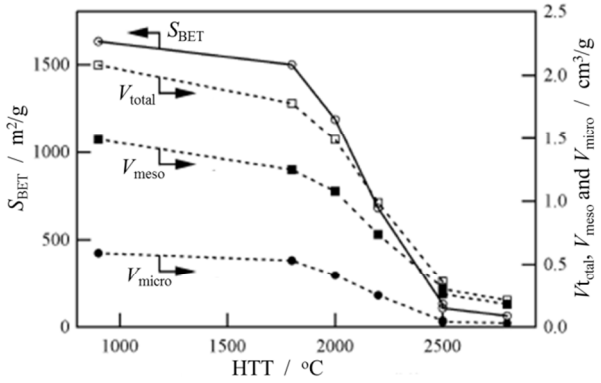

Fig. 12 Changes in S_{BET}, V_{total}, V_{micro} and V_{meso} with HTT for MgO-templated carbon. Reproduced from ref. 89 with permission.

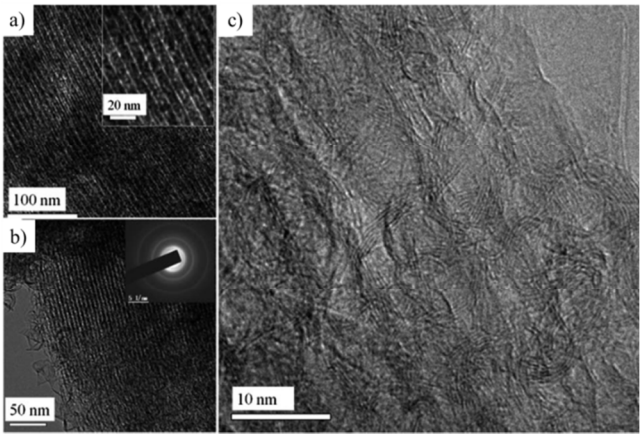

Fig. 13 Mesoporous carbon prepared by using CVD of CH_4 in silica template SBA at 900°C for 2.0 h (a) and for 3.0 h (b and c). Reproduced from ref. 92 with permission.

Microporous carbons have been prepared from various metal-carbides by their chlorination at high temperatures.[93] The carbon derived from titanium carbide at 600 °C was heat-treated at different temperatures of 1000-2000 °C for 2 h in high vacuum and studied by TEM, XRD and Ar adsorption.[94] TEM images of the carbon heat-treated at different temperatures and the change in XRD pattern with HTT is shown in Fig. 14. With increasing HTT, 002 fringes grow and become straight, but 002 diffraction profile is still very broad even after 2000 °C treatment. Above 1800 °C, 002 profile looks to be composite. As shown in Fig. 15, S_{BET} increases with increasing HTT up to 1500 °C, reaching 2085 m^2/g, and then rapidly decreases; correspondingly average pore size is constant at around 0.7 nm up to 1500 °C and then increases rapidly more than 2 nm.

Activated carbon fibers were prepared from poly(p-phenylene benzobisoxazole) (PBO) by carbonization at 900 °C, followed by CO_2 activation at 800 °C with two burn-off values of 15 and 51 mass%, and their pore structure variation with heat treatment at 1400-2700 °C was studied.[95,96] S_{BET} of the as-prepared carbon with burn-off of 51 mass% was 750 m^2/g but decreased to less than 2 m^2/g after 1600 °C treatment, although the crystalline structure was kept as turbostratic, d_{002} being 0.3448 nm. Crystallinity of PBO-derived carbon improved by the heat treatment at 2700 °C to give d_{002} of 0.3370-0.3372 nm, but its S_{BET} became negligibly small.

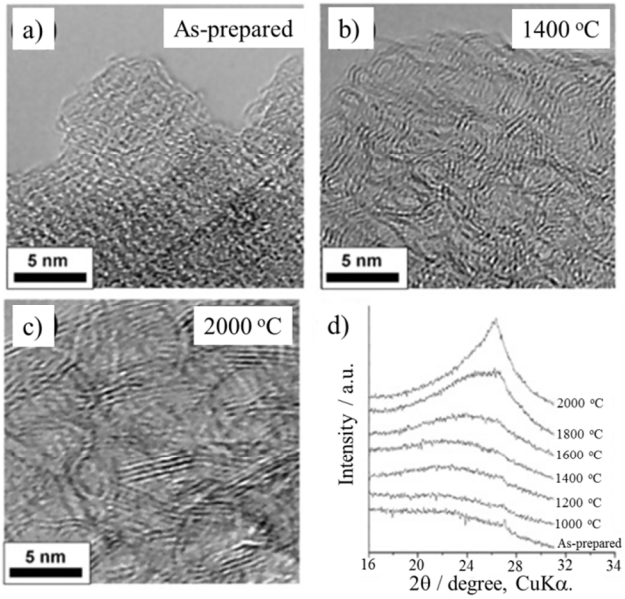

Fig. 14 TEM images and XRD patterns of carbide-derived carbon heat-treated at different temperatures. Reproduced from ref. 94 with permission.

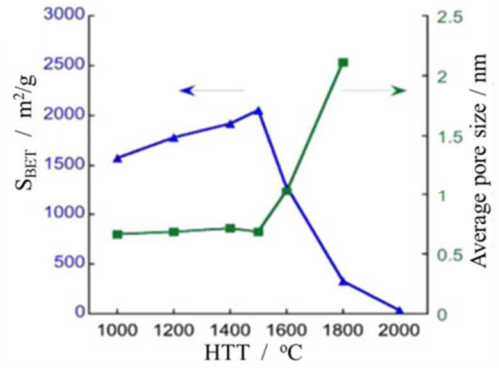

Fig. 15 Changes in S_{BET} and average pore size (a), and in Ar adsorption curve (b) with HTT for the microporous carbon derived from titanium carbide. Reproduced from ref. 94 with permission.

Heat treatment in molten sodium at 800 °C was carried out on activated carbon prepared from phenol/formaldehyde resin with or without manganese additives and followed by chemical activation to optimize the structure of porous carbon for electric double-layer capacitors.[97,98] The authors claimed that it is graphitization, but XRD patterns presented showed very broad 10 line, suggesting amorphous structure. Graphitization under high pressure (5 GPa) up to 1600 °C was performed on activated carbons.[99] The activated carbon having turbostratic structure was completely converted to graphite at the temperature above 1200 °C, associated with morphology change from granular to flaky.

3.2 Catalytic carbonization

Catalytic carbonization during the preparation of porous carbons has been proposed for various carbon precursors in order to give better crystallinity, consequently better electrical conductivity, to the resultant porous carbons.

Mesoporous carbons prepared from phenol resins via silica xerogel templating at 400-800 °C[100] was heat-treated at 900 °C for 3 h after impregnation of metal nitrate (Fe and Ni) in their ethanol solution, followed by the removal of metal particles with HCl.[101] Adsorption/desorption isotherms of nitrogen at 77 K show marked development of mesopores, associated with micropores, with increasing carbonization

temperature. The treatment of mesoporous carbons with metals was shown to be effective to increase electrical conductivity measured under the pressure of 7.1 MPa at room temperature, as shown for each carbon in Fig. 16. In comparison with the fact that the carbon heat-treated without metals have very low conductivity, $2x10^{-5}$ S/cm after 800 °C-treatment and 0.19 S/cm after 1200 °C-treatment, the conductivity is markedly improved by the heat-treatment at 900 °C with metals, more marked for the carbons carbonized at low-temperatures (400-500 °C) than those at high temperatures (600-800 °C).

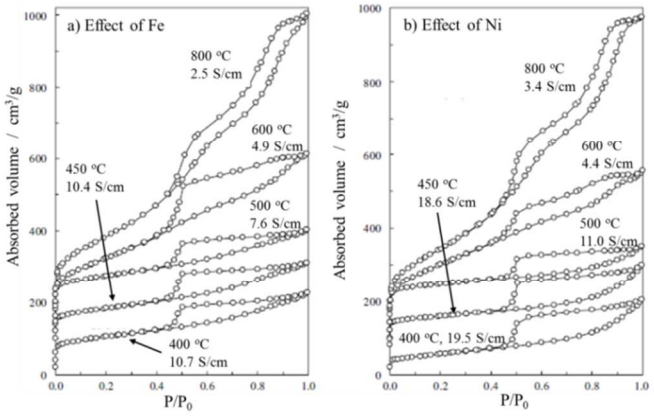

Fig. 16 Nitrogen adsorption/desorption isotherm for mesoporous carbon prepared at different temperatures, followed by the impregnation of either Fe (a) or Ni (b) and the heat-treatment at 900 °C. Heat treatment temperature and electrical resistivity are shown each sample. Reproduced from ref. 101 with permission.

Mesophase pitch mixed with $ZnCl_2$ and either $FeCl_3$ or $NiCl_2$ in organic solution was carbonized at 600-900 °C to obtain porous carbon, $ZnCl_2$ being expected to work as activation reagent and $FeCl_3$ and $NiCl_2$ as catalyst for the development of graphitic structure.[102] Electrical resistivity measured under the pressure of 10 MPa is plotted against carbonization temperature for the carbon obtained in Fig. 17. The carbon obtained by mixing with $ZnCl_2$ and $FeCl_3$ at the temperature below 800 °C gave S_{BET} of 600-860 m^2/g. By the carbonization at 900 °C, however, S_{BET} decreased to 275 m^2/g, though electrical resistivity decreased to about 1 Ωcm (conductivity of about 1 S/cm). The carbons obtained by mixing with $ZnCl_2$ and $NiCl_2$ showed low S_{BET} of 60-120 m^2/g, but relatively low resistivity of less than 1 Ωcm. The carbons carbonized at 900 °C showed composite 002 diffraction profile, showing the partial graphitization. The precursor fabricated by co-gelation of poly(furfuryl alcohol) with teraethylorthosilicate and a mixture of iron and cobalt nitrates was carbonized at 900 °C to prepare porous carbon.[103] The carbon obtained after the dissolution of SiO_2 and metal particles is supposed to have turbostratic structure from unsymmetrical 10 diffraction profile. 1,2,4,5-tetrakis(phenylethynyl)benzene as carbon precursor mixed with metal catalyst precursor ($Ni(CO)_2$, $Co_2(CO)_8$ or $Fe_2(CO)_9$) in methylene chloride solution was carbonized at 1000 °C to obtain porous carbon as the sorbent for ammonia vapor.[104]

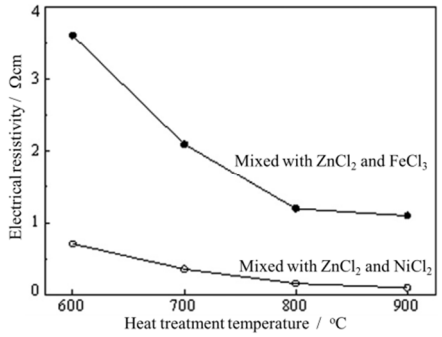

Fig. 17 Porous carbons prepared from mesophase pitch mixed with metal chlorides. Reproduced from ref. 102 with permission.

Porous carbons claiming to have graphitic structure were reported to be prepared by the carbonization of a carbon precursor mixed with a metal salt as catalyst precursor and template to produce nanopores at around 1000 °C.[105-115] Most of the resultant carbons, however, are supposed to have turbostratic structure from the experimental data reported, XRD, lattice fringe image of TEM and Raman spectroscopy. Via template carbonization using mesoporous silica (SBA-15) with nickel phthalocyanine at 800-900 °C, ordered mesoporous carbons composing of carbon layers were synthesized, which had S_{BET} of more than 1000 m^2/g and V_{total} of about 1 cm^3/g, but of which d_{002} was still 0.341-0.342 nm.[108] Nitrogen-doped mesoporous carbon was prepared by CVD of acetnitrile at 950-1100 °C in SBA-15.[105] Porous carbons with different morphologies were prepared from various complexes of ion-exchange resins with iron; nanocapsules from polyacrylic weak-base anion-exchange resin, nanoplatelets from polystyrenic strong-base anion-exchange resin, and nanosheets from polyacrylic weak-acid cation-exchange resin.[107] Mesoporous carbons were prepared from phenol/formaldehyde by using dual templating by polystyrene latex sphere and triblock copolymer F127 as template and Ni as catalyst in either N_2 or H_2/N_2 gas flow at 800 and 1000 °C.[109] The carbon obtained at 1000 °C in H_2/N_2 flow gave composite 002 diffraction profile having a component peak at 26.56 ° in 2θ (Cu Kα), suggesting the partial graphitization. Mesoporous

carbons prepared from phenol/formaldehyde with triblock copolymer P123 and ammonium ferric citrate gave electrical conductivity of $3.6x10^{-3}$-$12.6x10^{-3}$ S/cm under the pressure of 10 MPa.[111] Mesoporous carbons were prepared via F127 templating from resolcinol/formaldehyde precursor with Fe nanoparticles derived from Prussian blue at 600 °C.[112] The carbons prepared were claimed to be graphitized even after 600 °C treatment, but the XRD patterns showed obviously they have turbostratic structure, not yet graphitized. Melamine/formaldehyde with $CaCO_3$ nanoparticles gave porous carbons with S_{BET} of 834 m^2/g at 900 °C.[113] The carbons prepared above 1200 °C were partially graphitized, as revealed by the separation of 100 and 101 diffraction profiles in Fig. 18, with low porosity (S_{BET} of less than 84 m^2/g). Porous carbons were prepared from the xerogels of resolcinol/furfural resin with either $FeCl_3$ or $Ni(CH_3COO)_2$ at 1050 °C, which had d_{002} of 0.335-0.339 nm and S_{BET} of 158 m^2/g.[114] The carbon prepared from the xerogel with $FeCl_3$ at 1050 °C gave d_{002} of 0.337 nm, but S_{BET} of 171 m^2/g, and that with $CoCl_2$ gave 0.339 nm and 585 m^2/g, respectively.[115]

Hollow carbon nanocages were obtained from resorcinol/formaldehyde aerogels mixed with Cr, Fe, Co, Ni salts (1 mass% metal) by the carbonization at 1400-1800 °C.[116] They showed clear 002 lattice fringe images and d_{002} of about 0.337 nm was reported, although 002 diffraction profiles presented were composite. Similar carbon nanocages with a diameter of 30-50 nm were synthesized by the spray pyrolysis of ethanol solution of iron pentacarbonyl at 600-900 °C, which had relatively high S_{BET} as 800 m^2/g.[117,118] Iron nanoparticles formed from its carbonyl worked as the template to form nanocages and the catalyst to develop graphitic structure. By the addition of ammonium thiocyanate to ethanol solution of iron carbonyl, followed by the carbonization at 800 or 900 °C, smaller diameter and thinner wall of carbon nanocages were obtained.[119] By the decomposition of acetylene gas passing through liquid iron carbonyl at 1300 °C, carbon nanocages were obtained after the removal of metallic iron as iodide vapor at 1000 °C.[120] Iodine treatment was effective to increase both mesopores and micropores in the cage walls, in addition to remove iron. TEM images of carbon nanocages are shown in Fig. 19. Carbon nanocages are composed of well-oriented carbon layers, but their stacking is supposed to be still turbostratic from unsymmetrical 10 diffraction profile. Similar porous carbons were obtained at 900 °C from resorcinol/formaldehyde by using hydrated metal oxide particles (Fe, Ni and Mn) as template and catalyst.[121]

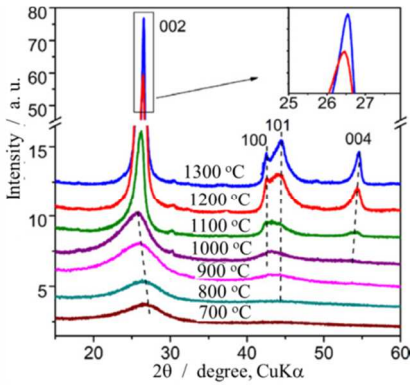

Fig. 18 Change in XRD pattern with carbonization temperature for carbon prepared from melamine/ formaldehyde with $CaCO_3$. Reproduced from ref. 113 with permission.

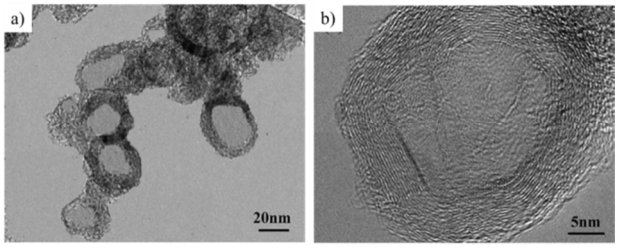

Fig. 19 Hollow carbon nanocages. Reproduced from ref. 120 with permission.

Carbon nanocoils were prepared from hydrothermal carbonization of saccharides (glucose, sucrose and starch) at 900-1000 °C after the deposition of either nickel or iron nitrate from its ethanol solution, followed by washing with HCl to remove metallic nickel particles and with $H_2SO_4/KMnO_4$ aqueous solution to remove amorphous carbon by oxidation.[122,123] The resultant nanocoils show clear 002 lattice fringe image, as shown in Fig. 20, but they have d_{002} of about 0.342 nm and unsymmetrical 10 profile of XRD,[124] suggesting the formation of turbostratic structure. Similar carbon nanocoils were obtained from resolcinol/formaldehyde mixed with nickel nitrate, cobalt nitrate and silica sol at 900 °C.[125] The resultant nanocoils look like to have a composite 002 diffraction profiles, one of component seeming to have graphitic structure because of relatively sharp and strong 101 diffraction peak, though the authors did not mention it.

Catalytic carbonization was studied on SiC with the catalyst, the mixture of equal amounts of $CoCl_2$, $NiCl_2$ and $FeCl_3$, by the heat treatment at 900-1100 °C in the flow of Cl_2 gas.[126] With increasing the content of the catalyst mixtures, S_{BET} and S_{micro} decrease, as shown in Fig. 21, S_{BET} from 1300 m^2/g for 0 mg/g to 300-500

m^2/g for 150 mg/g, although the improvement in crystallinity of carbon was not marked.

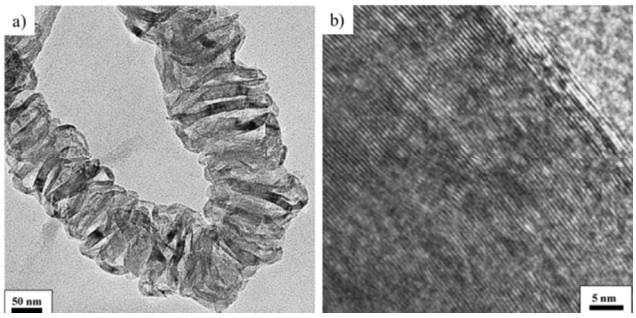

Fig. 20 Carbon nanocoils prepared from hydrothermally carbonized sucrose. Reproduced from ref. 124 with permission.

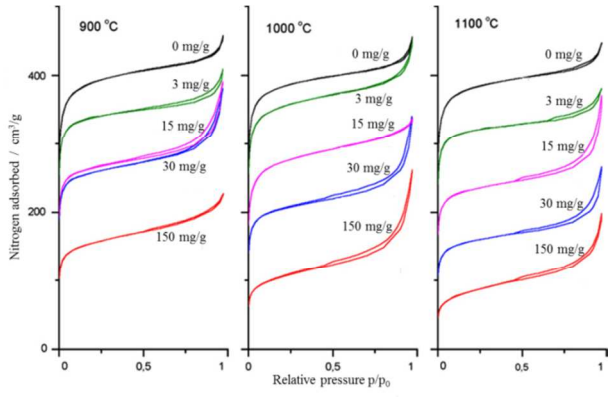

Fig. 21 Nitrogen adsorption/desorption isotherms of the carbons prepared from SiC withe different content of catalyst mixture ($CoCl_2$, $NiCl_2$ and $FeCl_3$) at 900-1100 °C. Reproduced from ref. 126 with permission.

4. Discussion

High temperature behavior in crystallinity of porous carbons is governed mainly by the precursor and not much by the process to control pore structure, although the precursors applicable for some processes are limited, non-fusible precursors for activation process, fusible precursors for the impregnation into some templates, etc. High temperature treatment of porous carbons is not desirable for keeping their porous structure. In most activated carbons, S_{BET} reduces to less than 10 % of the pristine after the heat treatment above 2000 °C (Fig. 6), in which no marked improvement in crystallinity is detected because of their non-graphitizing nature.[66,69.72,73] On carbon aerogels derived from resolcinol/formaldehyde, certain amount of mesopores are remained even after the heat treatment up to 2800 °C (Fig. 7), although micropores are disappeared above 2000 °C, but the crystallinity of the resultant porous carbons is not improved so much.[74] In mesoporous carbons derived from PVA via MgO templating, V_{meso} and V_{micro} decrease to 0.2 cm^3/g after the heat treatment above 2500 °C (Fig 12), although most of the particles of the resultant carbon changes to graphite structure.[89]

For the preparation of porous carbons via activation (activated carbons) from thermoplastic resins, a stabilization process is required to avoid plastic flow of the pyrolyzed carbonaceous products, of which the fundamental chemical reaction is oxidation using various reagents, and the resultant carbons become more or less non-graphitizing. In addition, the walls of porous carbons are thin, and give limited space for the development of graphite structure. Therefore, graphitization of porous carbons, no matter what precursor and what process being employed, is strongly required to be studied in more detail on crystalline structure, by taking consideration of the difference from bulky carbons, which have been studied in detail.

Nanoparticles of metals, such as Fe and Ni, have been mixed into carbon precursors via various processes aiming that they work as catalysts for graphitization. However, the experimental results published have not shown marked improvement in crystallinity of the resultant porous carbons. It has to be pointed out that the catalytic graphitization by these metals results in the formation of non-porous graphite particles separately from the pristine porous carbon particles. In some porous carbons, the formation of dense particles having graphite structure has been observed separately from porous particles after the treatment at high temperatures above 2000 °C, in a paper demonstrating by the analyses of XRD profiles and TEM images,[89] but in some papers suggesting by presenting composite 002 diffraction profiles.[69,72,79,86,94] The reason why this multiphase graphitization occurs in porous carbons has not been clearly understood, although most of them do not contain noticeable amount of metal impurities.

Associated with the improvement of crystallinity, electrical conductivity has been measured. Its measurement was performed under compression with various pressures[101,102] The measurement on a sheet prepared from porous carbons with a binder was also reported, looking forward their applications as the electrode materials for electrochemical capacitors and batteries.[89] It has to be pointed out that the detailed and comprehensive procedure for electrical resistivity

measurement on granular porous carbons has not been established.

5. Perspective

High crystallinity is one of effective processes for improving the functions, such as high electrical conductivity, thermal conductivity, catalytic activity, mechanical strength and oxidation resistance, for carbon, which can be reached by heat treatment at high temperatures, higher than 2000 °C. It has been well known that structural change in carbon materials at high temperatures depends predominantly on their precursor used.[1] For graphitizing carbons prepared from most of thermoplastic resins, including pitches, graphite structure starts to be developed above 2000 °C and its proportion, *i.e.*, graphitization degree, increases with increasing HTT. To have high degree of graphitization, in other words, to convert the principal structure to graphite, in which large enough hexagonal carbon layers stacked with three-dimensional regularity, the heat treatment above 2800 °C is required. On this graphitization process, so-called turbostratic structure is passed through, where hexagonal carbon layers grow relatively large but there is no regularity in their parallel stacking, and so it is pre-stage for developing three-dimensional graphite structure. For non-graphitizing carbons prepared from most of thermosetting resins, the development of graphite structure is usually very poor even after the heat treatment at 3000 °C.

Regrettably, no papers reporting on the crystallinity of porous carbons either by high temperature treatment or by catalytic carbonization have presented experimental data detailed enough with careful discussion. Many of them are saying that they prepared graphitic carbons, but no graphite structure is developed in their carbons prepared, just turbostratic structure being realized, as pointed out in the previous chapters, **2** and **3**. In these papers, the word "graphitic" does not mean the development of three-dimensional graphite structure, and it is supposed to mean that the carbons prepared are composed of small hexagonal carbon layers. However, we have to point out that almost all carbon materials consist of anisotropic hexagonal carbon layers, nevertheless small or extended, and also oriented or non-oriented, with very small numbers of exception, such as diamonds and fullerenes. The HTTs employed in many of the investigations are not wide enough and not high enough to discuss on the structure development in their porous carbons.

The systematic investigation is strongly desired on structural changes with a wide range of HTT (1400-3000 °C) on porous carbons prepared from different precursors (precursors giving graphitizing and non-graphitizing carbons) via each pore-controlling processes (activation, molecular structure control in organic precursors and various templating processes), where appropriate characterization on crystallinity and pore structure have to be included. The porous carbons thus characterized can be offered to the detailed studies on electrical, mechanical and chemical properties.

References

1 M. Inagaki, F. Kang, *Carbon Materials Science and Engineering -From Fundaments to Applications*, Tsinghua Univ. Press, Beijing, China 2011.
2 M. Inagaki, F. Kang, M. Toyoda, H. Konno, *Advanced Materials Science and Engineering of Carbon*, Elsevier & Tsinghua Univ. Press, Beijing, China 2013.
3 M. Inagaki, H. Konno, O. Tanaike, *J. Power Sources* **2010**, 195, 7880.
4 M.-X. Wang, Z.-H. Huang, K. Shen, F. Kang, K. Liang, *Catalysis Today* **2013**, 201, 109.
5 F. Rodriguez-Reinoso, *Introduction to Carbon Technologies,* Universidad de Alicante, Alicante, Spain 1997, Ch 2.
6 T. D. Burchell, *Carbon Materials for Advanced Technologies*, Pergamon, Amsterdam, Netherlands 1999.
7 M. Inagaki, C.-R. Park, J. M. Skowronski, A. W. Morawski, *Ads. Sci. Technol.* **2008**, 26, 735.
8 R. J. White, V. Budarin, R. Luque, J. H. Clark, D. J. Macquarrie, *Chem Soc. Rev.* **2009**, 38, 3401.
9 M. Inagaki, *New Carbon Mater.* **2009**, 24, 193.
10 B. Sakintuna, Y. Yurum, *Ind. Eng. Chem. Res.* **2005**, 44, 2893.
11 Y. Xia, Z. Yang, R. Mokaya, *Nanoscale* **2010**, 2, 639.
12 Y. Xia, Z. Yang, R. Mokaya, *Nanoscale* **2010**, 2, 639.
13 R. Fu, Z. Li, Y. Liang, F. Li, F. Xu, D. Wu, *New Carbon Mater.* **2011**, 26, 171.
14 A. D. Roberts, X. Li, H. Zhang, *Chem Soc. Rev.* **2014**, 43, 4341.
15 H. Marsh, D. S. Yan, T. M. O'Grady, A. Wennerberg, *Carbon* **1984**, 22, 603.
16 A. Linares-Solano, D. Lozano-Castello, M. A. Lillo-Rodenas, D. Cazorla-Amoros, *Chemistry and Physics of Carbon* Vol. 30, 2007, Ch. 1.

17 T. Nishikawa, M. Inagaki, *Adsorption Sci. Tech.* **2005**, 23, 827.
18 J. Jansta, F. P. Dousek, V. Patzelova, *Carbon* **1975**, 13, 377.
19 S. Shiraiashi, H. Kurihara, H. Tsuboi, A. Oya, Y. Soneda, Y. Yamada, *Electrochem. Solid State Lett.* **2001**, 4, A5.
20 M. Inagaki, N. Ohta, Y. Hishiyama, *Carbon* **2013**, 61, 1.
21 R. W. Pekala, C. T. Alviso, F. M. Kong, *J. Non-Cryst. Solids* **1992**, 145, 90.
22 Y. Hanzawa, K. Kaneko, *Langmuir* **1996**, 5, 7.
23 H. Hatori, Y. Yamada, M. Shiraishi, H. Nakata, S. Yoshitomi, *Carbon* **1992**, 30, 305.
24 H. Hatori, M. Shiraishi, H. Nakata, S. Yoshitomi, *Carbon* **1992**, 30, 719.
25 H. Sudo, K. Haraya, *J. Phys. Chem. B* **1997**, 101, 3988.
26 A. B. Fuertes, T. A. Centeno, *Microp. Mesop. Mater.* **1998**, 26, 23.
27 M. B. Coutinho, V. M. M. Salim, C. P. Borgees, *Carbon* 2003, 41, 1707.
28 C. W. Jones, W. J. Koros. *Carbon* **1994**, 32, 1419.
29 V. C. Geiszler, W. J. Koros, *Ind. Eng. Chem. Res.* **1996**, 35, 2999.
30 H. Kita, M. Yoshino, K. Tanaka, K. Okamoto, *Chem. Commun.* **1997**, 1051.
31 N. Ohta, Y. Nishi, T. Morishita, T. Tojo, M. Inagaki, *TANSO* **2008**, No. 233, 174.
32 N. Ohta, Y. Nishi, T. Morishita, T. Tojo, M. Inagaki, *Carbon* **2008**, 46, 1350.
33 Y. Yamada, O. Tanaike, T. T. Liang, H. Hatori, S. Shiraishi, A. Oya, *Electrochem. Solid-State Lett.* **2002**, 5, A283.
34 T. Kyotani, T. Nagai, S. Inoue, A. Tomita, *Chem. Mater*. **1997**, 9, 609.
35 T. Kyotani, *Carbon* **2000**, 38, 269.
36 B. Liu, H. Shioyama, T. Akita, Q. Xu, *J. Am. Chem. Soc.* **2008**, 130, 5390.
37 Y. Gogotsi, A. Nikitini, H. Ye, W. Zhou, J. E. Fischer, B. Yi, H. C. Foley, M. W. Barsoum, *Nat. Mater.* **2003**, 2, 591.
38 R. K. Dash, A. Nikitin, Y. Gogotsi, *Microp. Mesop. Mater.* **2004**, 72, 203.
39 J. Chmiola, G. Yushin, R. K. Dash, N. Hoffman, J. E. Fischer, M. W. Barsoum, Y. Gogotsi, *Electrochem. Solid-State Lett.* **2005**, 8, A357.
40 R. Ryoo, S. H. Joo, M. Kruk, M. Jaroniec, *Adv. Mater.* **2001**, 13, 677.
41 J. Lee, S. Han, T. Hyeon, *J. Mater. Chem.* **2004**, 14, 478.
42 C. Liang, K. Hong, G. A. Guiochon, J. W. Mays, S. Dai, *Angew. Chem. Int. Ed.* **2004**, 43, 5785.
43 S. Tanaka, N. Nishiyama, Y. Egashira, K. Ueyama, *Chem. Commun.* **2005**, 2125.
44 M. T. Gilbert, J. H. Knox, B. Kaur, *Chromatographia* **1982**, 16, 138.
45 S. Han, T. Hyeon, *Chem. Commun.* **1999**, 1955.
46 Z. J. Li, M. Jaroniec, *J. Am. Chem. Soc.* **2001**, 123, 9208.
47 Z. Li, M. Jaroniec, *Chem. Mater.* **2003**, 15, 1327.
48 J. Pang, X. Li, D. Wang, Z. Wu, V. T. John, Z. Yang, Y. Lu, *Adv. Mater.* **2004**, 16, 884.
49 T. Morishita, Y. Soneda, T. Tsumura, M. Inagaki, *Carbon* **2006**, 44, 2360.
50 T. Morishita, T. Tsumura, M. Toyoda, J. Przepiórski, A. W. Morawski, H. Konno, M. Inagaki, *Carbon* **2010**, 49, 2690.
51 W. F. Zhang, Z.-H. Huang, C. J. Zhou, G. Cao, F. Kang, Y. Yang, *J. Mater. Chem.* **2012**, 22, 7158.
52 J. Wang, *Electrochim. Acta* **1981**, 26, 1721.
53 A. G. Chakovskoi, C. E. Hunt, G. Forceberg, T. Nillson, P. Persson, *J. Vac. Sci. & Tech. B* **2003**, 21, 571.
54 M. Inagaki, T. Morishita, A. Kuno, T. Kito, M. Hirano, T. Suwa, K. Kusakawa, *Carbon* **2004**, 42, 497.
55 M. Kodama, J. Yamashita, Y. Soneda, H. Hatori, K. Kamegawa, *Carbon* **2007**, 45, 1105.
56 S. Chen, G. He, H. Hu, S. Jin, Y. Zhou, Y. He, S. He, F. Zhao, H. Hou, *Energy Environ. Sci.* **2013**, 6, 2435.
57 A. Stein, Z. Wang, M. A. Fierke, *Adv. Mater.* **2009**, 21, 265.
58 M. Inagaki, H. Orikasa, T. Morishita, *RSC Advances* **2011**, 1, 1620.
59 H. Nishihara, T. Kyotani, *Adv. Mater.* **2012**, 24, 4473.
60 T. Kyotani, A. Tomita, *J. Jpn. Petrol. Inst.* **2002**, 45, 261.
61 A. Janes, L. Permann, M. Arulepp, E. Lust, *Electrochem. Commun.* **2004**, 6, 313.
62 J. Hu, H. Wang, Q. Gao, H. Guo, *Carbon* **2010**, 48, 3599.
63 B. Liu, H. Shioyama, H. Jiang, X. Zhang, Q. Xu, *Carbon* **2010**, 48, 456.
64 H.-L. Jiang, B. Liu, Y.-Q. Lan, K. Kuratani, T. Akita, H. Shioyama, F. Zong, Q. Xu, *J. Am. Chem. Soc.* **2011**, 133, 11854.
65 T. Morishita, L. Wang, T. Tsumura, M. Toyoda, H. Konno, M. Inagaki, *TANSO* **2010**, No. 242, 60 [in Japanese].
66 Y. Toda, N. Yuki, S. Toyoda. *Carbon* **1972**, 10, 13.
67 S. K. Verma, P. L.Walker Jr, *Carbon* **1990**, 28, 175.

68 Z. Kowalczyk, J. Sentek, S. Jodzis, R. Diduszko, A. Presz, A. Terzyk, Z. Kucharski, J. Suwalski, *Carbon* **1996**, 34, 403.
69 S. Błazewicz, A. Swiatkowski, B. J. Trznadel, *Carbon* **1999**, 37, 693.
70 M. Kang, Y.-S. Bae, C.-H. Lee, *Carbon* **2005**, 43, 1512.
71 T. X. Nguyen, S. K. Bhatia, *Carbon* **2006**, 44, 646.
72 J. Rodriguez-Mirasol, T. Cordero, J. J. Rodriguez, *Carbon* **1996**, 34, 43.
73 R. Gadiou, A. Didion, S.-E. Saadallah, M. Couzi, J.-N. Rouzaud, P. Delhaes, C. Vix-Guter, *Carbon* **2006**, 44, 3348.
74 Y. Hanzawa, H. Hatori, N. Yoshizawa, Y. Yamada, *Carbon* **2002**, 40, 575.
75 X. Wang, C. Liang, S. Dai, *Langmuir* **2008**, 24, 7500.
76 S.-H. Chai, J. Y. Howe, X. Wang, M. Kidder, V. Schwartz, M. L. Golden, S. H. Overbury, S. Dai, D. D. Jiang, *Carbon* **2012**, 50, 1574.
77 Y. Tian, Y. Song, Z. Tang, Q. Guo, L. Liu, *J. Power Sources* **2008**, 184, 675.
78 Z. Tang, Y. Song, Y. Tian, L. Liu, Q. Guo, *Microp. Mesop. Mater.* **2008**, 111, 48.
79 C. L. Burket, R. Rajagopalan, H. C.Foley, *Carbon* **2007**, 45, 2307.
80 C. L. Burket, R. Rajagopalan, H. C. Foley, *Carbon* **2008**, 46, 501.
81 Z. Li, M. Jaroniec, Y.-J. Lee, L. R. Radovic, *Chem. Commun.* **2002**, 1346.
82 S. B. Yoon, G. S. Chai, S. K. Kang, J.-S. Yu, K. P. Gierszal, M. Jaroniec, *J. Am. Chem. Soc.* **2005**, 127, 4188.
83 H. Yamada, Y. Watanabe, I. Moriguchi, T. Kudo, *Solid State Ionics* **2008**, 179, 1706.
84 F. Zeng, Z. Hou, B. He, C. Ge, J. Cao, Y. Kuang, *Mater. Res. Bull.* **2012**, 47, 2104.
85 C. Vix-Guterl, S. Saadallah, L. Vidal, M. Reda, J. Parmentier, J. Patarin, *J. Mater. Chem.* **2003**, 13, 2535.
86 A. B. Fuertes, S. Alvarez, *Carbon* **2004**, 42, 3049.
87 M. Inagaki, S. Kobayashi, F. Kojin, N. Yanaka, T. Morishita, B. Tryba, *Carbon* **2004**, 42, 3153.
88 K. Shen, Z.-H. Huang, L. Gan, F. Kang, *Chem. Lett.* **2009**, 38. 90.
89 H. Orikasa, T. Morishita, *TANSO* **2012**, No. 254, 1 [in Japanese].
90 Y. Soneda, T. Yamaguchi, K. Imoto, M. Kodama, T. Morishita, H. Orikasa, *TANSO* **2013**, No. 256, 57 [in Japanese].
91 T. Tsumura, A. Arikawa, T. Kinumoto, Y. Arai, T. Morishita, H. Orikasa, M. Inagaki, M. Toyoda, *Mater. Chem. Phys.* **2014**, 147, 1175.
92 Z. Wu, W. Li, Y. Xia, P. Webley, D. Zhao, *J. Mater. Chem.* **2012**, 22, 8835.
93 V. Presser, M. Heon, Y. Gogotsi, *Adv. Funct. Mater.* **2011**, 21, 810.
94 S. Osswald, J. Chmiola, Y. Gogotsi, *Carbon* **2012**, 50, 4880.
95 M. B. Vazquez-Santos, A. Martinez-Alonso, J. M. D. Tascon, J. N. Rouzaud, E. Geissler, K. Laszlo, *Carbon* **2011**, 49, 2960.
96 M. B. Vazquez-Santos, E. Geissler, K. Laszlo, J.-N. Rouzaud, A. Martinez-Alonso, J. M. D. Tascon, *Carbon* **2012**, 50, 2929.
97 Z. Xu, D. Cai, Z. Hu, F. Wang, L. Gan, *Electrochim. Acta* **2014**, 117, 486.
98 Z. Xu, D. Cai, Z. Hu, L. Gan, *Microp. Mesop. Mater.* **2014**, 195, 36.
99 J. Zhao, L. Yang, F. Li, R. Yu, C. Jin, *Carbon* **2009**, 47, 744.
100 A. B. Fuertes, *Chem. Mater.* **2004**, 16, 449.
101 M. Sevilla, A. B. Fuertes, *Carbon* **2006**, 44, 468.
102 D. Zhai, H. Du, B. Li, Y. Zhu, F. Kang, *Carbon* **2011**, 49, 725.
103 Z. Wang, X. Zhang, X .Liu, M. Lu, K. Yang, J. Meng, *Carbon* **2011**, 49, 161.
104 J. W. Long, Laskoski, W. Peterson, T. M. Keller, K. A. Pettigrew, B. J. Schindler, *J. Mater. Chem.* **2011**, 21, 3477.
105 Y. Xia, R. Mokaya, *Adv. Mater.* **2004**, 16, 1553.
106 A.-H. Lu, W.-C. Li, E.-L. Salabas, B. Spliethoff, F. Schuth, *Chem. Mater.* **2006**, 18, 2086.
107 L. Wang, C. Tian, B. Wang, R. Wang, W. Zhou, H. Fu, *Chem. Commun.* **2008**, 5411.
108 T. K. Lee, X. Ji, M. Rault, L. F. Nazar, *Angew. Chem. Int. Ed.* **2009**, 48, 5661.
109 C. Huang, R. Dong, D. Gu, D. Zhao, *Carbon* **2011**, 49, 3055.
110 N. Zhao, S. Wu, C. He, C. Shi, E. Liu, X. Du, J. Li, *Mater. Lett.* **2012**, 87, 77.
111 A. Wang, J. Ren, B. Shi, G. Lu, Y. Wang, *Microp. Mesop. Mater.* **2012**, 151, 287.
112 N. P. Wickramaratne, V. S. Perera, B.-W. Park, M. Gao, G. W. McGimpsey, S. D. Huang, M. Jaroniec, *Chem. Mater.* **2013**, 25, 2803.
113 G. Yang, H. Han, T. Li, C. Du, *Carbon* **2012**, 50, 3753.
114 W. Kicinski, M. Norek, M. Bystrzjewski, *J. Phys. Chem. Solids* **2013**, 74, 101.
115 W. Kicinski, M. Bystrzejewski, M. H. Ruemmeli, T. Gemming, *Bull. Mater. Sci.* **2014**, 37, 141.
116 F. J. Maldonado-Hodar, C. Moreno-Castilla, J. Rivera-Utrilla, Y. Hanzawa, Y. Yamada, *Langmuir* **2000**, 16, 4367.

117 J. N. Wang, Y. Z. Zhao, J. J. Niu, *J. Mater. Chem.* **2007**, 17, 2251.
118 J. N. Wang, L .Zhang, J. J. Niu, F. Yu, Z. M. Sheng, Y. Z. Zhao, H. Chang, C. Pak, *Chem. Mater.* **2007**, 19, 453.
119 B. Y. Xia, J. N. Wang, X. X. Wang, J. J. Niu, Z. M. Sheng, M. R. Hu, Q. C. Yu, *Adv. Funct. Mater.* **2008**, 18, 1790.
120 S. J. Teng, X. X. Wang, B. Y. Xia, J. N. Wang, *J. Power Sources* **2010**, 195, 1065.
121 J. Li, R. Lu, B. Dou, C. Ma, Q. Hu, Y. Liang, F. Wu, S. Qiao, Z. Hao, *Environ. Sci. Technol.* **2012**, 46, 12648.
122 M. Sevilla, C. Sanchıs, T. Valdes-Solıs, E. Morallon, A. B. Fuertes, *Carbon* **2008**, 46, 931.
123 M. Sevilla, G. Lotta, A. B. Fuertes, *J. Power Sources* **2007**, 171, 546.
124 M. Sevilla, A. B. Fuertes, *Mater. Chem. Phys.* **2009**, 113, 208.
125 V. Celorrio, L. Calvillo, M. V. Martınez-Huerta, R. Moliner, M. J. Lazaro, *Energy Fuels* **2010**, 24, 3361.
126 M. Kaarik, M. Arulepp, M. Karelson, J. Leis, *Carbon* **2008**, 46, 1579.